Nanoscale

COMMUNICATION

View Article Online
View Journal | View Issue

Cite this: *Nanoscale*, 2014, **6**, 2567

Received 1st November 2013
Accepted 29th November 2013

DOI: 10.1039/c3nr05840a

www.rsc.org/nanoscale

Large-area fabrication of highly reproducible surface enhanced Raman substrate *via* a facile double sided tape-assisted transfer approach using hollow Au–Ag alloy nanourchins†

Zhen Liu,[a] Lin Cheng,[a] Lei Zhang,[a] Chao Jing,[b] Xin Shi,[b] Zhongbo Yang,[a] Yitao Long[b] and Jixiang Fang*[a]

Ideally, a SERS substrate should possess super signal amplification, high uniformity and reproducibility. Up to now, an emphasis on reproducibility and uniformity has been crucial to ensure consistent chemical detection sensitivity across the surface of a SERS substrate. Here we demonstrate a simple and facile double sided tape-assisted transfer method to fabricate surface enhanced Raman scattering (SERS) substrates with prominent performance using hollow Au–Ag alloy nanourchins (HAAA-NUs). Such a large area, closely-packed flat film of the HAAA-NUs with a high density of "hot spots" exhibits a high SERS activity and reproducibility, simultaneously. The AFM-correlated nano-Raman and the point by point scanning of SERS signals verify the excellent spatial uniformity and reproducibility with a low relative standard deviation (RSD) less than 15% using crystal violet as probe molecule at the concentrations of 1×10^{-8} M and 1×10^{-10} M. The SERS signals of Sudan dye at a 1×10^{-8} M concentration also show high reproducibility with a low RSD of 13.8%. This facile protocol presented here could lead to a high quality SERS substrate and open tremendous potential for various applications.

Introduction

Since the discovery of the SERS effect on roughed silver electrode surface,[1] many studies have been conducted to explore diverse promising SERS substrates. Currently, most investigations have been focused on exploring various nanostructures with different shapes, sizes and nanogaps between nanoparticles so as to achieve high SERS detection sensitivity.[2–5] The studies on the reproducibility and uniformity of SERS signals are centralized on advanced top-down nanopatterning techniques such as electron beam lithography, optical lithography, nanoimprint lithography, nanosphere lithography, and so on.[6–9] However, these techniques have limitations regarding throughput, cost and fabrication of well-controlled small gaps of a few nanometers or complex nanostructures to create efficient "hot spots". Thus only a moderate SERS enhancement factor, *e.g.* $\sim 10^5$–10^6 is usually obtained.[10] Therefore, the key point to ensure reliability and sensitivity in biological and chemical detection focuses on the fabrication of uniform, highly sensitive and spatially reproducible SERS substrates.[11,12]

Up to now, although various nanoparticles with well-controlled shapes and sizes have been synthesized, self-assembly *via* droplet evaporation with suspended nanoparticles on a solid surface, as the simplest and cost-saving method, has not yet been successfully exploited to prepare highly efficient SERS substrates. On the one hand, the self-assembly of colloidal nanoparticles on a substrate with free defects over a large area is still hard to achieve, partially because of induced capillary flow.[13,14] Thus the assembled area was not large enough for a highly reproducible and uniform SERS substrate. On the other hand, in order to prepare an orderly close-packed array *via* the self-assembly during the solvent evaporation, polymer or organic ligands were always employed,[15,16] which unavoidably affect the subsequent absorption of detected molecules onto the surface of plasmonic nanoparticles, thus resulting in the loss of SERS sensitivity. Therefore, how to fabricate a high quality SERS substrate using the various obtained nanostructures remains a technical challenge.

When a drop of colloidal suspension dries on a surface, it leaves behind coffee rings or clumps due to the dewetting of the solvent during the self-assembly process (Scheme 1a and b). Recently, some modified droplet evaporation methods, such as two-stage control,[17] suspended drying droplet,[18] drying in a Teflon ferrule,[19] *etc.*, have been reported. However, the cracks, clumps or empty bands, were still not eliminated. When the thickness of the film can be increased by increasing the concentration of nanoparticle suspension or by multiple feeding of the droplet (Scheme 1c), the cracks, clumps or empty bands may be significantly reduced within the continuous thick film. In this situation, the top surface of the film may still

[a]*State Key Laboratory for Mechanical Behavior of Materials, School of Science, Xi'an Jiaotong University, Xi'an, Shaanxi, 710049, P. R. China. E-mail: jxfang@mail.xjtu.edu.cn; Tel: +86 29 82665995*

[b]*Key Laboratory for Advanced Materials, Department of Chemistry, East China University of Science and Technology, Shanghai, 200237, P. R. China*

† Electronic supplementary information (ESI) available: Fig. S1–S6. See DOI: 10.1039/c3nr05840a

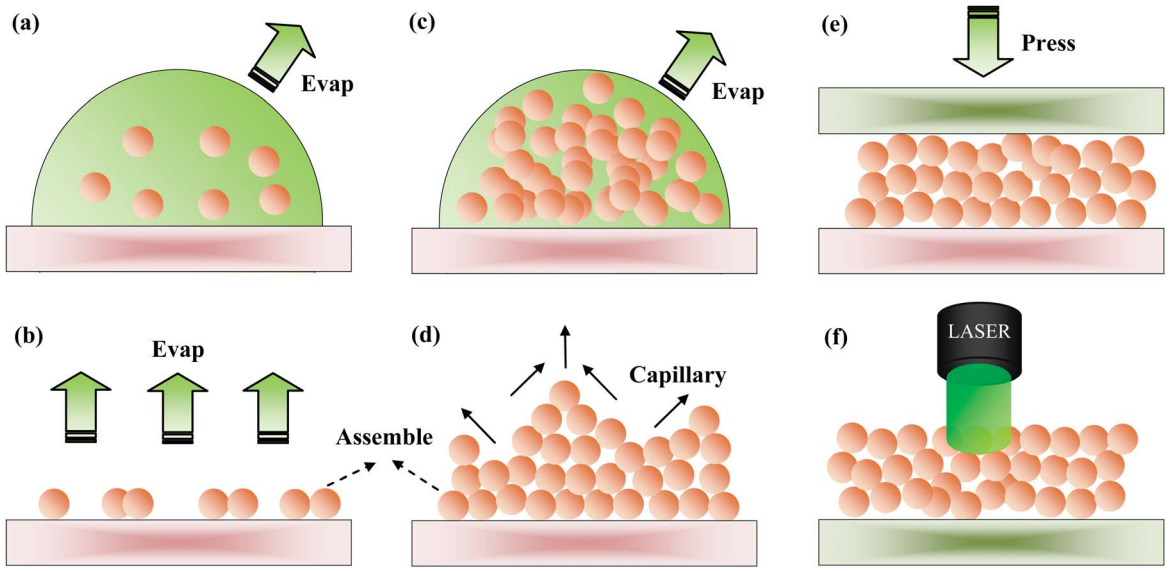

Scheme 1 Schematic plots of solvent evaporation and double sided tape-assisted film transformation. The formation of a film with (a) and (b) a thin layer, (c) and (d) a thick layer, (e) the double sided tape-assisted film transformation process, (f) SERS detection of the obtained inverted surface.

demonstrate the coffee-stain-like rings or highly rough topography owing to the uneven radial velocity distribution of fluid (Scheme 1d).[20] However, the bottom surface of the thick film may be flat consisting of highly closed-packed nanoparticles. Therefore, if a film transfer approach is employed to reverse the top/bottom surface of the film, then a smooth surface may be used as the high quality SERS substrate (Scheme 1e and f).

In this paper, we demonstrate a simple and facile double sided tape-assisted transfer method to fabricate surface enhanced Raman scattering (SERS) substrates with prominent performance. The hollow Au–Ag alloy nanourchins (HAAA-NUs) were synthesized *via* a seed-mediated route[21–24] (see Experimental section and ESI†) and used in this study. The sea-urchin like nanoparticles with multiple tips have demonstrated an ultrahigh SERS sensitivity which has been certified by Raman detection and finite-difference time-domain method (FDTD) simulations.[25] We take advantage of the high SERS detection sensitivity and the excellent uniformity of transferred film by simply dropping the HAAA-NUs onto a glass substrate, to make excellent SERS substrates with high Raman sensitivity and reproducibility, simultaneously. This method may be applied to fabricate SERS substrates using nanostructures with different shapes, sizes, and materials. Thus, this double sided tape-assisted transfer strategy describes a facile and novel scheme to fabricate large-area, highly sensitive and reproducible SERS substrates.

Experimental section

Fabrication of SERS substrate using HAAA-NUs

The procedure for fabricating the flat film *via* the HAAA-NUs by means of the double sided tape-assisted method (Scheme 2) includes three steps. *Step-i*, the thick layer deposition of the HAAA-NUs. Firstly, a glass sheet was cleaned sequentially with aqua regia once, DI water twice, and ethanol twice under ultrasonic irradiation and dried in air. The as-prepared HAAA-NUs were washed with HCOOH (500 mM) once, ammonia solution once and DI three times in turn, and then redispersed in 100–500 μl water. Here the HAAA-NUs suspension was used to form a thick layer of HAAA-NUs by dropping a certain amount of the clean HAAA-NU suspension onto the glass substrate, drying it in air and repeating the dropping and drying procedure two or three times. The formation of a thick layer with almost no interstices was to improve the quality of the final product. It is noted that we also attempted to disperse the

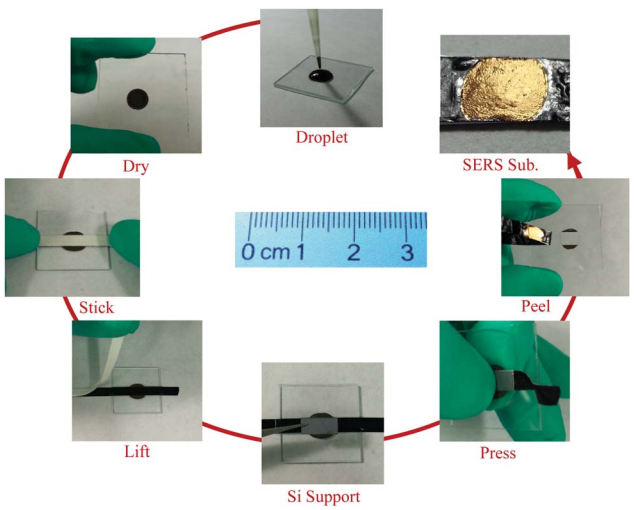

Scheme 2 Flow-process diagram of the procedures for fabricating SERS substrate using HAAA-NUs by double sided tape-assisted film transformation method.

HAAA-NUs in ethanol to shorten the evaporation time of the dispersing agent. But it was hard to form a complete thick layer. The HAAA-NUs aggregated automatically along with the evaporation of solvent. The different wettability of water and ethanol, and the capillary phenomenon between the dispersing agents and the HAAA-NUs, lead to different results. *Step-ii*, the transformation of the thick layer. First a piece of double sided tap was stuck on the top of the thick layer. Then the cleaned Si wafer was put on the tape right above the deposits to serve as a support after lifting the release paper from the tape. The Si support was pressed gently several times by hand. Then the tape was peeled off from the glass substrate slowly to protect the film from breakage. Thus the HAAA-NU layer was transferred onto the Si substrate and the HAAA-NUs aggregated SERS substrate was obtained. In this step, we use the double sided conductive tape usually employed in routine scanning electron microscope (SEM) testing because this tape is thick and strong enough for peeling the deposits off the glass sheet. We can also choose different tapes to adjust the area of the SERS substrate to meet the diverse requirements of analysis. The smoothness of the tape has a great influence on the flatness of the obtained substrate. So we could improve the quality of the substrate by using more flat tape. Additionally, we gently press the Si wafer above the deposits to ensure the complete transformation of the thick layer to the Si wafer. What we should pay attention to is that too much pressure can lead to the HAAA-NUs getting squashed (see Fig. S2†). Furthermore, the glass sheet can be replaced by a Si wafer or something else with relatively flat surface to deposit the HAAA-NUs. *Step-iii*, cleaning the obtained substrate. Rinse the substrate with DI water for one minute, and then dry it at room temperature.

Results and discussion

Characterization of HAAA-NUs and HAAA-NUs assembly

The HAAA-NUs appear to have an ultrahigh density of sharp tips, *i.e.* about 100 tips within a single ~100 nm nanourchin (Fig. 1a). The tips and the nanogaps between the roots of the tips may display an ultrahigh density of hot spots (the inset of Fig. S1†). Additionally, the formation of Au–Ag alloy may improve the SERS sensitivity and stability in contrast to pure Au and Ag nanostructures.[26,27] The dark-filled image and the corresponding scattering spectra of the HAAA-NUs measured in air are shown in Fig. 1b and c, displaying an obvious surface plasmonic absorption band around 650 nm (Fig. 1c). Furthermore, the peaks of scattering spectra for diverse individual HAAA-NUs demonstrate no obvious difference. The ultraviolet-visible (UV) spectrum measured in DI water (Fig. S1†) indicated the wide tunable capability of localized surface plasmon resonances (LSPRs) for the suspension of HAAA-NUs.

The different magnified SEM images of the substrate (Fig. 2) fabricated *via* the above described process (see Scheme 2) display its large-area flatness. The area of the flat film on the tape (Fig. 2a) is around 5 mm × 5 mm. For the demand of larger substrate in practical applications, we need larger tape in the fabrication process. Meanwhile, we also present the photographs of substrates fabricated at different times (Fig. S3†) by means of the double sided tape-assisted method. It is seen that there are some defects such as cracks and pinholes on the flat substrates (Fig. 2a and S3†). The width of the cracks is >2 μm that could be easily observed during the Raman detection. The small pinholes are about several tens to ~200 nm in size (Fig. 2b–d). As shown in Fig. 2b–d, the morphology of the HAAA-NUs remains the same as that before deposition. In addition, a great number of tips within the individual HAAA-NU and the overlapping of the adjacent HAAA-NUs within the closely-packed film could create strong plasmonic coupling between tips. Thus, Fig. 2 displays a uniform large-scale deposited surface as well as closely-packed microstructure consisting of individual HAAA-NUs and gaps between HAAA-NUs.

SERS of HAAA-NUs assembly

In order to investigate the uniformity of SERS signals, two techniques were adopted including AFM-correlated nano-Raman and the point by point scanning mode. The study of SERS performance was carried out with crystal violet (CV) as the probe molecule. The as-fabricated substrates were treated by UV Ozone for 4 h without heating, submerged in CV aqueous

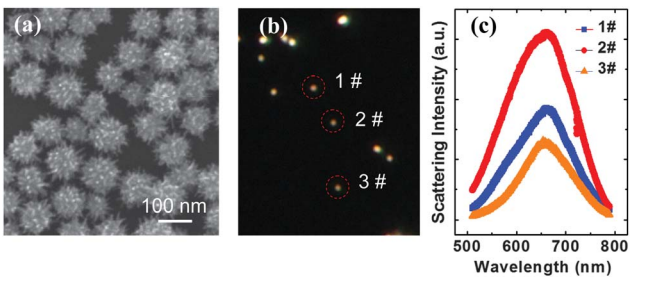

Fig. 1 (a) SEM image of HAAA-NUs; (b) dark-field scattering image; and (c) scattering spectra of HAAA-NUs measured in air.

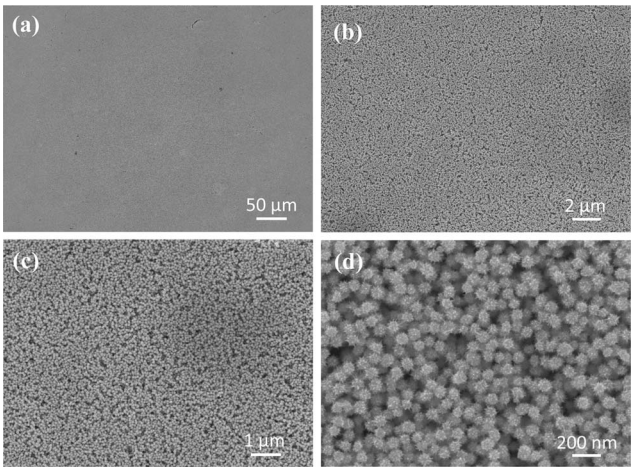

Fig. 2 (a) Low magnified SEM image of the SERS substrate with ~0.4 mm in width and ~0.5 mm in length; (b)–(d) different magnified SEM images of the SERS substrate.

solution of various concentrations for 8 h, and then gently rinsed in DI water for 1 min, and made it dry in the air. Using a 532 nm diode laser, the AFM-correlated nano-Raman was performed by mapping the characteristic Raman peak of CV at 1172 cm^{-1} with a step size of 156 nm and a scan area of 10 μm × 10 μm. The obtained AFM image (Fig. 3a) reflects the large-area dense arrangement of the HAAA-NUs. There are some pinholes in quite a few areas. The depth of the pinholes is <500 nm according to the height profile (Fig. 3c) scanned along the line as shown in the AFM image (Fig. 3a). Unexpectedly, the SERS image presents a relatively uniform distribution of SERS signals even for the pinhole regions marked by the circles in the AFM image (Fig. 3a). This phenomenon indicates that the AFM tip may not enter into the small nanogaps which contribute a huge enhancement. Meanwhile, the pinholes have a weak influence on the uniformity of the SERS signal owing to the size of pinholes still being within the '*z*' resolution of Raman spectroscopy.

The point by point scanning spectra of CV molecule at the concentration of 10^{-8} M were recorded with steps of 2 μm (Fig. 4a), a 633 nm excitation laser and a laser spot diameter of 0.85 μm. The resulting 3D waterfall plot of SERS spectra (Fig. 4b) obtained by mapping the 20 μm × 20 μm area (see Fig. 4a) reveals the high uniformity of Raman signals. For all of the 100 spots, each spot exhibits a high capability to enhance the Raman signal of the CV molecules. To quantitatively assess the reproducibility of the SERS signals, the intensities of the 100 spots concerning the characteristic vibration of CV at 1172 cm^{-1} were collected (Fig. 4c). According to the statistics (Fig. 4c), the calculated relative standard deviation (RSD) of the Raman vibration at 1172 cm^{-1} is 12.5%, revealing the exceptional uniformity of the as-prepared substrate. Additionally, it is seen that 93% intensity of the SERS signals are within the limits of

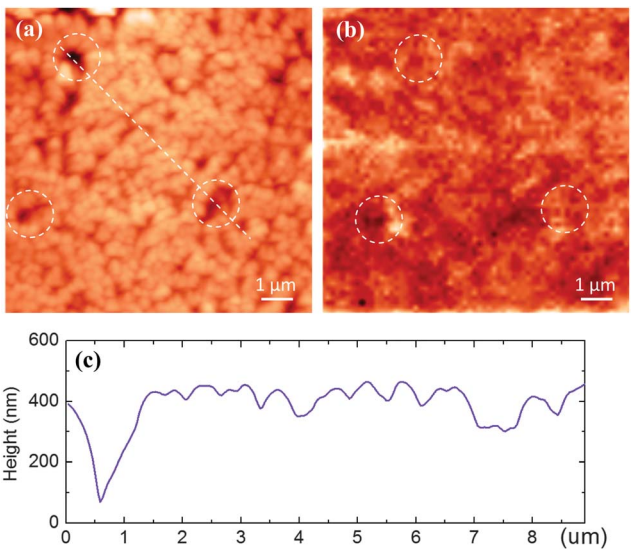

Fig. 3 (a) Atomic force micrograph of flat film fabricated *via* HAAA-NUs; (b) corresponding nano-Raman image obtained from 532 nm excitation laser; (c) the height profile of the HAAA-NU film along the line shown in the AFM image.

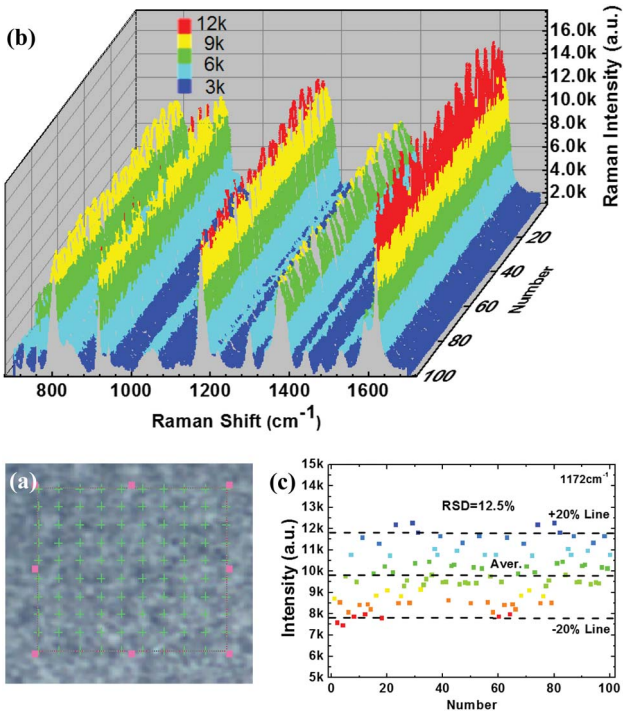

Fig. 4 (a) Optical images of flat film obtained *via* double sided tape-assisted film transformation method; (b) SERS spectra obtained from the point by point scanning of the area shown in (a) measured by a 633 nm excitation laser; (c) the intensity of the main Raman vibrations of CV at the concentration of 10^{-8} M.

the ±20% deviation of the average intensity of signals. The low value of RSD, the narrowly distributed and high intensities of SERS signals indicate the as-prepared substrate may be a promising substrate for highly sensitive and uniform SERS detection.[28]

To further evaluate the uniformity and sensitivity of the substrate under a lower concentration (*e.g.* 1 × 10^{-10} M) of probe molecule, we study the SERS performance of other identical substrates. The detection was performed in three different regions of 10 μm × 10 μm in size marked by A, B and C in Fig. 5a. The point by point SERS detection was performed with a larger laser spot of 1.5 μm and a same step size of 2 μm. The 3D waterfall plot of SERS spectra of the three corresponding areas (Fig. 5a) are shown in Fig. 5b–d, respectively. We also calculated the statistics of the Raman intensity distribution at 1172 cm^{-1} for the three regions (Fig. 5e). From Fig. 5b–e, it can be seen that the Raman signals of the three regions are relatively uniform with RSD values of 11.9%, 14.9% and 9.8%, respectively. Most Raman densities of the spots in the three regions are within the bounds of ±20% of the average signal, which further certifies the high performance of the SERS substrates.[28] However, the top surface of the thick layer shows a relatively large RSD value of 20.8% (Fig. S4†), which further verifies the advantage of the current method. Fig. S5† is the comparison of the top and bottom surfaces obtained by the current route. The SEM images clearly display an obvious morphological difference between both sides, which is consistent with the RSD

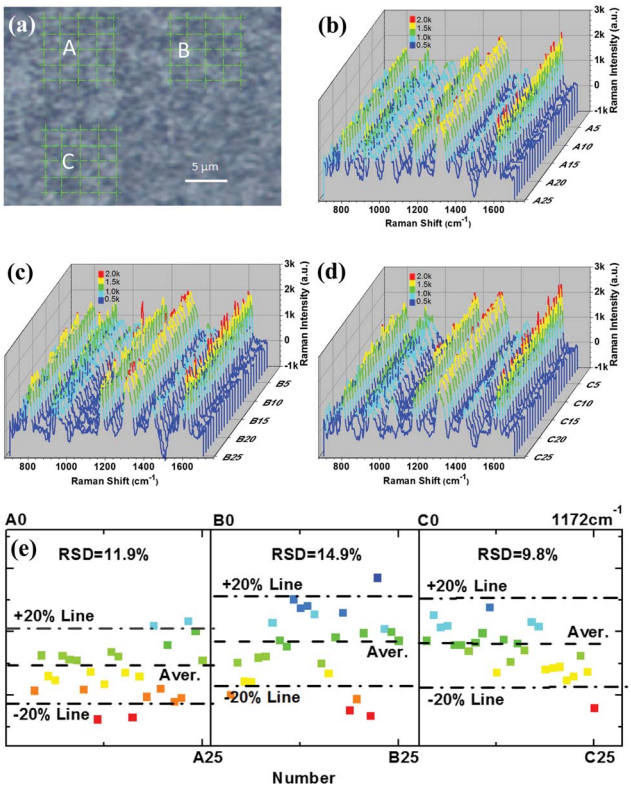

Fig. 5 (a) Optical image of the flat film obtained *via* the double sided tape-assisted film transformation method; (b)–(d) SERS spectra obtained from the point by point scanning of the three regions shown in (a) measured by a 633 nm excitation laser; (e) the intensity of the main Raman vibrations of CV molecule at the concentration of 10^{-10} M.

values obtained from the top side and bottom side. In this study, we have also expanded the current method to other practical applications such as in food safety. Fig. S6† shows Raman spectra of Sudan I (SDI) dye detected with a 0.85 μm spot size, which shows also a good uniformity with a RSD value of 13.8%.

Among various factors, the laser spot size used in the Raman measurement and the density of nanogaps, as well as the concentration of dye molecule, are of importance to achieve a good uniformity of SERS detection. Basically, the larger laser spot size we use the better uniformity we obtain. For example, Schmidt, *et al.* reported a <10% deviation from the average signals for the leaned silicon pillar array when a laser spot diameter of 3.1 μm was used.[29] Meanwhile, increasing the density of nanogaps, particularly at the ultralow concentration of the probe molecule, is greatly beneficial to obtain a uniform SERS signal.[29,30] In this study, the SERS performance fabricated *via* the double sided tape-assisted method by using HAAA-NUs is remarkable. On the one hand, owing to the small size of HAAA-NUs, a 0.85 μm laser spot could cover almost seventy of ~100 nm HAAA-NUs ($\pi \times (850/2)^2/(\pi \times (100/2)^2)$). Over two hundred of ~100 nm HAAA-NUs were included when the laser spot became 1.5 μm in size. At the concentration of 1×10^{-8} M of CV, we obtained the RSD of less than 15% (*i.e.* 12.5%) with a 0.85 μm spot size (×100 objective lens). Furthermore, at a lower concentration of CV, *e.g.* 1×10^{-10} M, a small RSD of less than 15% was also obtained using a 1.5 μm (×50 WL) objective lens. Therefore, in practical SERS applications, to detect unknown molecules at an ultra-low concentration, substrates with a high density of hotspots combined with a large laser spot will help to achieve more consistent SERS signals. On the other hand, compared with the smooth spherical nanoparticles, the individual HAAA-NU possesses abundant hotspots.[25,31] Meanwhile, the interparticle interactions of the adjacent HAAA-NUs may also contribute to additional hot spots, thus leading to an enhanced uniformity of the SERS signals. Therefore, the obtained SERS substrate in this work displays an improved uniformity and reproducibility with a RSD of less than 15%. This value is remarkable compared with substrates fabricated by other approaches such as electron beam lithography,[32,33] capillary-assisted route,[9,19,34] polymer-mediated methods,[35,36] organic monolayer assisted way,[37] and *in situ* formed SERS substrates.[38,39]

Conclusions

In summary, the double sided tape-assisted film transformation method was successfully used to fabricate an excellent SERS substrate by simply dropping the HAAA-NUs onto a glass substrate. The AFM-correlated nano-Raman images demonstrate a flat surface and homogeneous SERS signal of the corresponding region. Meanwhile the point to point scanning spectra of CV molecule at 10^{-8} M and 10^{-10} M demonstrated high reproducibility and uniformity with less than 15% RSD. The low RSD variation demonstrates the as-fabricated flat film is appropriate for highly sensitive SERS detection. In addition, this novel procedure to fabricating SERS substrate is free of organic and inorganic impurities. Therefore, the substrates exhibited outstanding sensitivity, uniformity in SERS measurement and may be well-suited for chemicals' detection, food safety and environmental monitoring.[40–42]

Acknowledgements

J. X. Fang was supported by National Natural Science Foundation of China (no. 51171139), the Tengfei Talent Project of Xi'an Jiaotong University, the New Century Excellent Talents in University (NCET), Scientific New Star Program in Shaanxi Province (no. 2012KJXX-03), Doctoral Fund of Ministry of Education of China (nos 20110201120039, 20130201110032) and the Fundamental Research Funds for the Central Universities (no. 08142008).

References

1 M. Fleischman, P. Hendra and A. McQuillan, *Chem. Phys. Lett.*, 1974, **26**, 123–126.
2 J. F. Li, Y. F. Huang, Y. Ding, Z. L. Yang, S. B. Li, X. S. Zhou, F. R. Fan, W. Zhang, Z. Y. Zhou, D. Y. Wu, B. Ren, Z. L. Wang and Z. Q. Tian, *Nature*, 2010, **464**, 392–395.

3 X. H. Li, G. Y. Chen, L. B. Yang, Z. Jin and J. H. Liu, *Adv. Funct. Mater.*, 2010, **20**, 2815–2824.
4 D. K. Lim, K. S. Jeon, J. H. Hwang, H. Kim, S. Kwon, Y. D. Suh and J. M. Nam, *Nat. Nanotechnol.*, 2011, **6**, 452–460.
5 D. K. Lim, K. S. Kim, J. M. Nam and Y. D. Suh, *Nat. Mater.*, 2010, **9**, 60–67.
6 L. Polavarapu and Q. H. Xu, *Langmuir*, 2008, **24**, 10608–10611.
7 Y. Lu, G. L. Liu, J. Kim, Y. X. Mejia and L. P. Lee, *Nano Lett.*, 2005, **5**, 119–124.
8 T. Chen, H. Wang, G. Chen, Y. Wang, Y. H. Feng, W. S. Teo, T. Wu and H. Y. Chen, *ACS Nano*, 2010, **4**, 3087–3094.
9 R. H. Que, M. W. Shao, S. J. Zhou, C. Y. Wen, S. D. Wang and S. T. Lee, *Adv. Funct. Mater.*, 2011, **21**, 3337–3343.
10 H. Ko, S. Singamaneni and V. V. Tsukruk, *Small*, 2008, **4**, 1576–1599.
11 D. He, B. Hu, Q. F. Yao, K. Wang and S. H. Yu, *ACS Nano*, 2009, **3**, 3993–4002.
12 A. Kim, F. S. Qu, D. A. A. Ohlberg, M. Hu, R. S. Williams and Z. Y. Li, *J. Am. Chem. Soc.*, 2011, **133**, 8234–8239.
13 X. M. Lin, H. M. Jaeger, C. M. Sorensen and K. J. Klabunde, *J. Phys. Chem. B*, 2001, **105**, 3353–3357.
14 K. Keseroglu and M. Culha, *J. Colloid Interface Sci.*, 2011, **360**, 8–14.
15 T. P. Bigioni, X. M. Lin, T. T. Nguyen, E. I. Corwin, T. A. Witten and H. M. Jaeger, *Nat. Mater.*, 2006, **5**, 265–270.
16 H. Wang, C. S. Levin and N. J. Halas, *J. Am. Chem. Soc.*, 2005, **127**, 14992–14993.
17 Y. Xie, S. M. Guo, C. F. Guo, M. He, D. X. Chen, Y. H. Ji, Z. Y. Chen, X. C. Wu, Q. Liu and S. S. Xie, *Langmuir*, 2013, **29**, 6232–6241.
18 S. Keskin and M. Culha, *Analyst*, 2012, **137**, 2651–2657.
19 A. Q. Chen, A. E. Deprince, A. Demortiere, A. Joshi-Imre, E. V. Shevchenko, S. K. Gray, U. Welp and V. K. Vlasko-Valsov, *Small*, 2011, **7**, 2365–2371.
20 P. P. Fang, J. F. Li, Z. L. Yang, L. M. Li, B. Ren and Z. Q. Tian, *J. Raman Spectrosc.*, 2008, **39**, 1679–1687.
21 K. G. M. Chow, *J. Nanopart. Res.*, 2012, **14**, 1186–1205.
22 L. L. Zhao, K. Ding, X. H. Ji, J. Li, H. L. Wang and W. S. Yang, *Colloids Surf., A*, 2011, **386**, 172–178.
23 X. M. Lu, H. Y. Tuan, J. Y. Chen, Z. Y. Li, B. A. Korgel and Y. N. Xia, *J. Am. Chem. Soc.*, 2007, **129**, 1733–1742.
24 J. Y. Chen, M. X. Yang, Q. Zhang, E. C. Cho, C. M. Cobley, C. H. Kim, C. Glaus, L. H. V. Wang, M. J. Welch and Y. N. Xia, *Adv. Funct. Mater.*, 2010, **20**, 3684–3694.
25 J. X. Fang, S. Y. Du, S. Lebedkin, Z. Y. Li, R. Kruk, M. Kappes and H. Hahn, *Nano Lett.*, 2010, **10**, 5006–5013.
26 M. Rycenga, C. M. Cobley, J. Zeng, W. Y. Li, C. H. Moran, Q. Zhang, D. Qin and Y. N. Xia, *Chem. Rev.*, 2011, **111**, 3669–3712.
27 T. Guo and Y. W. Tan, *Nanoscale*, 2013, **5**, 561–569.
28 S. Q. Wang, L. P. Xu, Y. Q. Wen, H. W. Du, S. T. Wang and X. J. Zhang, *Nanoscale*, 2013, **5**, 4284–4290.
29 M. S. Schmidt, J. Hübner and A. Boisen, *Adv. Mater.*, 2012, **24**, OP11–OP18.
30 C. Mu, J. P. Zhang and D. S. Xu, *Nanotechnology*, 2010, **21**, 15604–15610.
31 S. K. Pandian, P. S. Isabel, R. G. Benito, F. J. G. Abajo and M. L. M. Luis, *Nanotechnology*, 2008, **19**, 15606–15612.
32 N. A. Abu Hatab, J. M. Oran and M. J. Sepaniak, *ACS Nano*, 2008, **2**, 377–385.
33 Q. M. Yu, P. Guan, D. Qin, G. Golden and P. M. Wallace, *Nano Lett.*, 2008, **8**, 1923–1928.
34 F. S. Ou, M. Hu, I. Naumov, A. Kim, W. Wu, A. M. Bratkovsky, X. M. Li, R. S. Williams and Z. Y. Li, *Nano Lett.*, 2011, **11**, 2538–2542.
35 J. C. Heckel, L. M. Kisley, J. M. Mannion and G. Chumanov, *Langmuir*, 2009, **25**, 9671–9676.
36 M. K. K. Oo, C. F. Chang, Y. Z. Sun and X. D. Fan, *Analyst*, 2011, **136**, 2811–2817.
37 X. Zhou, F. Zhou, H. L. Liu, L. B. Yang and J. H. Liu, *Analyst*, 2013, **138**, 5832–5838.
38 X. H. Tang, W. Y. Cai, H. B. Yang and J. H. Liu, *Nanoscale*, 2013, **5**, 11193–11199.
39 Q. Q. Ding, H. L. Liu, L. B. Yang and J. H. Liu, *J. Mater. Chem.*, 2012, **22**, 19932–19939.
40 Y. D. Wang, N. Lu, W. T. Wang, L. X. Liu, L. Feng, Z. F. Zeng, H. B. Li, W. Q. Xu, Z. J. Wu, W. Hu, Y. Q. Lu and L. F. Chi, *Nano Res.*, 2013, **6**, 159–166.
41 Y. Q. Wen, W. Q. Wang, Z. L. Zhang, L. P. Xu, H. W. Du, X. J. Zhang and Y. L. Song, *Nanoscale*, 2013, **5**, 523–526.
42 Z. L. Zhang and Y. Q. Wen, *Appl. Phys. Lett.*, 2012, **101**, 173109–173113.

